The use of the 3-21G basis though shows how eventually the results become somewhat erratic if we cut back too far on the basis set. For reaction 6 the difficulty with treating H_2 is again apparent from the much better agreement in Table IX for the forward than the reverse barrier at the MP2 and MP–SAC2 levels. This is improved somewhat at the MP4 and MP–SAC4 levels of theory. For the latter, the forward barrier is roughly the same as that predicted by the much larger basis sets (Table VII), while the reverse barrier is about 2 kcal/mol higher than the more accurate results. Nonetheless, it is important to recognize that the MP–SAC4/3-21G results for this reaction are better than those predicted by any of the much more expensive unextrapolated MP2 or MP4 values in Table VII. As an example of the difference in computing time, the Cray-1 CPU time required for the MP4/3-21G calculations at the transition state is 14 s, which is much less than that for MP4 calculations with the 6-31G(2p,d) basis, 323 s.

For reaction 7 the MP2 corrections for the forward and reverse barriers are rather large. As a result, SAC2 underestimates the forward barrier (the predicted interaction energy is actually negative at the SCF/3-21G saddle-point geometry) and may be fortuitously accurate for the backward one. At the MP–SAC4/3-21G level, the forward barrier is within the range of experimental estimates, while the reverse barrier is much too small. Nonetheless, whereas both MP2/3-21G and MP4/3-21G calculations predict the energy difference for the overall reaction to have the wrong sign, the MP–SAC2/3-21G and MP–SAC4/3-21G calculations both, remarkably, remove this error. Nevertheless, it appears to be asking too much of the extrapolation procedure to predict an accurate berrier height for a case where the unextrapolated ΔE has such a large error.

VII. Concluding Remarks

The concept of scaling all the correlation energy, as estimated by *n*th-order Møller–Plesset perturbation theory (MP–SAC*n*), has been advanced and tested for the class of processes in which bonds to H are made and broken. Even using standard basis sets, the method is very promising and should allow for improved estimates of bond dissociation energies and reaction barrier heights. Use of specially balanced basis sets may lead to even greater accuracy and allow the method to be extended to wider classes of processes.

The MP–SAC method is an economical way to improve the accuracy of ab initio electronic structure calculations, thereby turning them into advanced semiempirical methods. For example, the semiempirical MP–SAC2 method with medium-size basis sets, which involves the same computational labor as the ab initio MP2 method, is often more accurate than the more computationally demanding ab initio MP4 method with much larger basis sets. We conclude that the SAC method should be of widespread usefulness for improving the accuracy of electronic energies in cases where multi-configuration reference states are not essential.

Acknowledgment. The authors are grateful to Rozeanne Steckler for helpful assistance. This work was supported in part by the National Science Foundation under Grant No. CHE83-17944 and CHE83-09948 and the Air Force Office of Scientific Research under Grant No. 82-0190 and by the University of Minnesota Supercomputer Institute.

Registry No. $CH_3^{\bullet}$, 2229-07-4; CH_4, 74-82-8.

Peptide Plane Orientations Determined by Fundamental and Overtone ^{14}N NMR

R. Tycko, P. L. Stewart, and S. J. Opella*

Contribution from the Department of Chemistry, University of Pennsylvania, Philadelphia, Pennsylvania 19104. *Received November 5, 1985*

Abstract: A method for determining the orientations of peptide planes in single crystal or uniaxially oriented samples is presented. The method depends on the measurement of multiple orientationally dependent spectroscopic parameters in solid state fundamental and overtone ^{14}N NMR experiments. Results are presented from experiments on a single crystal sample of *N*-acetyl-D,L-valine, in which there are two magnetically inequivalent molecular orientations. The spectroscopic data are analyzed in terms of the orientations of peptide planes with respect to the direction of the applied magnetic field, taking into account experimental error and uncertainties in the nuclear spin interaction tensors. The peptide plane orientations determined by ^{14}N NMR and by X-ray diffraction for *N*-acetylvaline are in close agreement.

The three-dimensional structure of a molecule can be established from intramolecular distances, intramolecular angles, or a combination of distances and angles. X-ray diffraction measurements yield the relative positions of individual atoms, from which the relative orientations of chemical groups such as peptide planes can be determined. NMR cross relaxation measurements on biopolymers in solution yield internuclear distances,[1] which can be combined with the known structures of the chemical groups to determine molecular conformations.[2,3] Solid state NMR techniques, as described in this paper, directly yield angular measurements. The angles between nuclear spin interaction tensors and the direction of the applied magnetic field can be determined in oriented samples from spectroscopic measurements of the frequencies and splittings of the anisotropic chemical shift, nuclear quadrupole, and dipole–dipole interactions. When the orientations of the spin interaction tensors in the molecular framework are known, the spectroscopic measurements can be used to extract the angles between chemical groups and the field direction. The orientations of peptide planes can in principle be determined by two independent angular measurements. If the orientations of individual peptide planes in a polypeptide are known, then the secondary and tertiary backbone structures can be constructed by using standard bond lengths and geometries.

The observation of nitrogen NMR resonances is useful for the determination of peptide plane orientations because each peptide bond contains an amide nitrogen. Previous work has relied on ^{15}N labeling to enable ^{15}N NMR experiments,[4-7] but the alter-

(1) Jeener, J.; Meier, B. H.; Bachmann, P.; Ernst, R. R. *J. Chem. Phys.* **1979**, *71*, 4546–4553.
(2) Braun, W.; Wider, G.; Lee, K. H.; Wuthrich, K. *J. Mol. Biol.* **1983**, *169*, 921–948.
(3) Kline, A. D.; Braun, W.; Wuthrich, K. *J. Mol. Biol.* **1986**, *189*, 377–382.
(4) Cross, T. A.; Opella, S. J. *J. Am. Chem. Soc.* **1983**, *105*, 306–308.
(5) Cross, T. A.; Tsang, P.; Opella, S. J. *Biochemistry* **1983**, *22*, 721–726.

0002-7863/86/1508-5419$01.50/0

native approach of ^{14}N NMR has several advantages. ^{14}N NMR does not require isotopic labeling. The ^{14}N quadrupole interaction of peptide linkages offers high spectral and orientational resolution because of the large magnitude of the quadrupole coupling constant and asymmetry parameter.[8-16] The combination of cross-polarization[17] and the 99% abundance of ^{14}N means that sensitivity is high. We have recently implemented ^{14}N overtone NMR[18,19] which is complementary to conventional single quantum (fundamental)[8-16] and double quantum[20-24] ^{14}N NMR. The combination of fundamental and overtone ^{14}N techniques provides advantages in both the experimental and interpretive aspects of the spectroscopy. In particular, ^{14}N overtone NMR has the advantage over fundamental NMR of having a total spectral width of approximately 120 kHz (for amide nitrogens in a 5.9 T field) rather than the 4.8 MHz spectral width of fundamental ^{14}N NMR.[18,19] This greatly enhances the practicality of the spectroscopy. On the other hand, fundamental ^{14}N spectra have the advantages of higher sensitivity and resolution. The combination of multiple independent structural measurements from overtone and fundamental ^{14}N NMR spectra improves the accuracy and precision of the results.

In the conventional solid state ^{14}N NMR spectrum of an oriented or single crystal sample, each unique orientation of a nitrogen site contributes two fundamental resonances centered near the Larmor frequency. The splitting between the two resonances is a function of the orientation of the ^{14}N quadrupole interaction tensor with respect to the magnetic field direction and may be as large as 4.8 MHz for amide ^{14}N nuclei. In addition, the midpoint of the two resonances is shifted from the isotropic Larmor frequency by the second order quadrupole shift and, to a lesser degree, by chemical shift anistropy. Each amide nitrogen has a heteronuclear dipole coupling with the bonded proton that further splits each fundamental resonance into a doublet in undecoupled spectra. The size of the splitting due to the heteronuclear dipole coupling is a function of the angle between the N–H bond and the applied magnetic field.

^{14}N overtone NMR spectra have a single resonance for each unique nitrogen orientation. The overtone resonance is shifted from twice the Larmor frequency by twice the second order shift plus twice the chemical shift. Like the quadrupole splitting, the second order quadrupole shift is orientationally dependent. Heteronuclear dipole splittings can be observed in overtone spectra. In addition, the nutation frequency of an overtone transition under rf irradiation is a function of the molecular orientation.

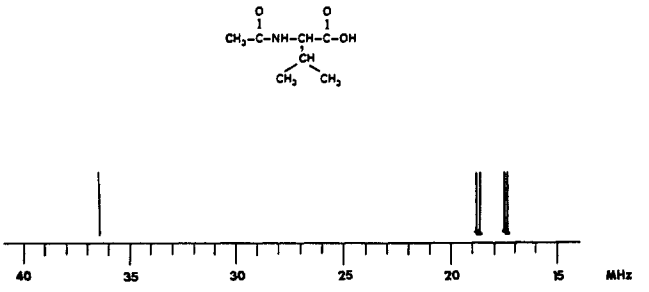

Figure 1. The complete ^{14}N NMR spectrum of a single crystal of *N*-acetyl-D,L-valine. The fundamental transitions give rise to the two doublets near the 18.061-MHz Larmor frequency. The overtone transitions give rise to two single resonances near twice the Larmor frequency of 36.122 MHz.

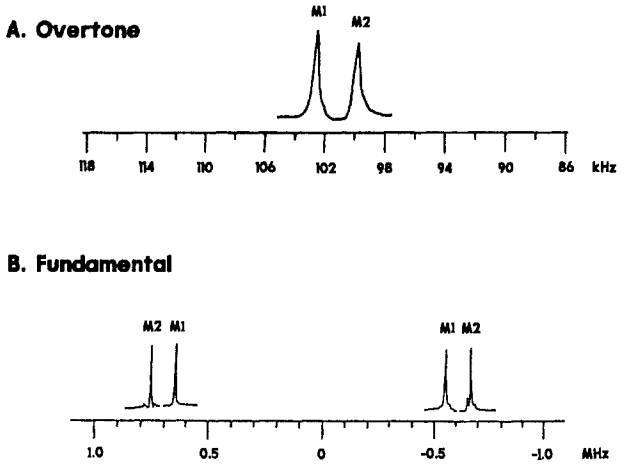

Figure 2. Expansions of the overtone (A) and fundamental (B) spectral regions from Figure 1. The resonances for the two inequivalent molecular orientations in the crystal are labeled M1 and M2. The frequency scales represent offsets from 36.122 MHz (A) and 18.061 MHz (B). The overtone spectrum was acquired with 2000 transients; the fundamental spectrum was obtained in four spectral windows, with 500 transients in each.

In this paper, we show how the orientationally dependent spectral parameters that are measured in fundamental and overtone ^{14}N NMR experiments can be interpreted in terms of the orientation of individual peptide planes relative to the magnetic field direction. The approach is demonstrated on a single crystal of *N*-acetylvaline, which contains molecules with two magnetically distinct peptide plane orientations.[11] Experimental measurements are carried out at a single arbitrary orientation of the crystal. A graphical method for analyzing the results of multiple experiments in terms of molecular orientations is presented. The peptide plane orientations determined by ^{14}N NMR are compared to those determined by X-ray diffraction.

Experimental Section

The NMR experiments were carried out on a homebuilt double resonance spectrometer with a 5.9 T magnetic field. All experiments were performed at room temperature on a single 50-mg crystal of *N*-acetyl-D,L-valine. A probe that could be tuned to both the fundamental and the overtone ^{14}N transitions was used, allowing all measurements to be performed without moving the crystal or the probe. Both the fundamental and the overtone spectra were obtained with cross-polarization,[17] by using proton spin locking for fundamental cross-polarization and proton dipolar order for overtone cross-polarization. Proton-decoupled spectra were obtained with 1.2 mT decoupling fields.

Results

Figure 1 contains the complete ^{14}N NMR spectrum of a single crystal of *N*-acetylvaline. The same orientation of the crystal was used in all of the experiments. The presence of two inequivalent *N*-acetylvaline molecules is readily seen in the spectrum. The two molecular orientations give rise to two symmetrical doublets

(6) Cross, T. A.; Frey, M. H.; Opella, S. J. *J. Am. Chem. Soc.* **1983**, *105*, 7741–7743.
(7) Cross, T. A.; Opella, S. J. *J. Mol. Biol.* **1985**, *182*, 367–381.
(8) Blinc, R.; Mali, M.; Osredkar, R.; Prelesnik, A.; Zupancic, I. *J. Chem. Phys.* **1971**, *55*, 4843–4848.
(9) Blinc, R.; Mali, M.; Osredkar, R.; Prelesnik, A.; Zupancic, I. *Chem. Phys. Lett.* **1971**, *9*, 85–87.
(10) Wolff, E. K.; Griffin, R. G.; Watson, C. *J. Chem. Phys.* **1977**, *66*, 5433–5438.
(11) Stark, R. E.; Haberkorn, R. A.; Griffin, R. G. *J. Chem. Phys.* **1978**, *68*, 1996–1997.
(12) Griffin, R. G.; Bodenhausen, G.; Haberkorn, R. A.; Huang, T. H.; Munowitz, M.; Osredkar, R.; Ruben, D. J.; Stark, R. E.; van Willigen, H. *Philos. Trans. R. Soc. London, A* **1981**, *299*, 547–563.
(13) Haberkorn, R. A.; Stark, R. E.; van Willigen, H.; Griffin, R. G. *J. Am. Chem. Soc.* **1981**, *103*, 2534–2539.
(14) Naito, A.; Ganapathy, S.; Raghunathan, P.; McDowell, C. *J. Chem. Phys.* **1983**, *79*, 4173–4182.
(15) Naito, A.; Barker, P.; McDowell, C. *J. Chem. Phys.* **1984**, *81*, 1583–1591.
(16) Naito, A.; McDowell, C. *J. Chem. Phys.* **1984**, *81*, 4795–4803.
(17) Pines, A.; Gibby, M. G.; Waugh, J. S. *J. Chem. Phys.* **1972**, *56*, 1776–1777.
(18) Tycko, R.; Opella, S. J. *J. Am. Chem. Soc.* **1986**, *108*, 3531–3532.
(19) (a) Bloom, M., private communication. (b) Legros, M., M. Sc. Thesis, University of British Columbia, 1984. (c) Creel, R. B.; Von Meerwall, E. D.; Barnes, R. G. *Chem. Phys. Lett.* **1977**, *49*, 501–503.
(20) Vega, S.; Shattuck, T. W.; Pines, A. *Phys. Rev. Lett.* **1976**, *37*, 43–46.
(21) Vega, S.; Pines, A. *J. Chem. Phys.* **1977**, *66*, 5624–5644.
(22) Vega, S.; Shattuck, T. W.; Pines, A. *Phys. Rev. A* **1980**, *22*, 638–661.
(23) Brunner, P.; Reinhold, M.; Ernst, R. R. *J. Chem. Phys.* **1980**, *73*, 1086–1094.
(24) Reinhold, M.; Brunner, P.; Ernst, R. R. *J. Chem. Phys.* **1981**, *74*, 184–188.

Table I. Summary of Spectroscopic Measurements

parameter	molecule M1	molecule M2
quadrupole splitting (fundamental)	1.191 MHz	1.424 MHz
obsd shift (overtone)	103 kHz	100 kHz
obsd shift (fundamental)	51.5 kHz	50.0 kHz
second-order quadrupole shift	52.5 kHz	51.0 kHz
chemical shift[a]	−57 ppm (−1.0 kHz)	−57 ppm (−1.0 kHz)
N–H dipole splitting (overtone)	15.7 kHz	15.7 kHz
N–H dipole splitting (fundamental)	7.9 kHz	7.9 kHz
relative nutation frequency (overtone)	0.073	0.060

[a] The chemical shifts are calculated by using eq 5 and the final peptide plane orientations in Figure 10. The values $\sigma_{\parallel} = 114$ ppm and $\sigma_{\perp} = -57$ ppm are used.

centered near the ^{14}N Larmor frequency of 18.061 MHz. These are the fundamental transitions. The overtone transitions appear as two single resonances that are shifted slightly from twice the Larmor frequency (36.122 MHz). The two overtone resonances cannot be distinguished on the frequency scale of Figure 1 but can be resolved in the expanded spectrum in Figure 2. Because of the wide frequency separation of the fundamental transitions caused by the large quadrupole coupling constant of the nitrogen sites in peptide linkages, each of the fundamental resonances had to be obtained with a separate measurement after retuning the probe and resetting the rf carrier frequency. In contrast, both of the overtone resonances were obtained in a single spectrum.

The large difference in spectral widths for the fundamental and overtone spectra is illustrated in Figure 2. These two spectra are shown on frequency scales that differ by an order of magnitude, reflecting the difference in magnitude of the first- and second-order quadrupole effects. Each line in the spectra in Figure 2 is labeled M1 or M2 to indicate from which of the two inequivalent molecular orientations it arises. The quadrupole splittings and total observed frequency shifts, i.e., second-order quadrupole shifts plus chemical shifts, can be measured directly from the spectra in Figure 2. In a crystal of *N*-acetylvaline with only two inequivalent peptide plane orientations, the fundamental spectrum in Figure 2B can be used to measure both the first order quadrupole splitting and the total shift for each ^{14}N nuclei, since the two fundamental resonances of each nucleus are shifted equally. In more complex fundamental spectra, it may be difficult to identify the pair of resonances that correspond to a single site in order to measure the shift accurately. The shifts can be measured independently and directly in the overtone spectra. This is demonstrated in Figure 2A. The main contribution to the total observed shift is the second order quadrupole shift, which may be as large as 60 kHz under the conditions of these experiments. The contribution of chemical shift anistropy is at most 3 kHz.[26] Both contributions are considered in the analysis of the data presented below.

The magnitude of the N–H heteronuclear dipole coupling can be measured in both the fundamental and overtone spectra with either one- or two-dimensional spectroscopy. Two-dimensional methods are required when there is extensive overlap of resonances. Only rarely will overlap be a problem in the fundamental spectrum because of the large spectral width resulting from the quadrupole splittings. Two-dimensional experiments are more typically needed in overtone NMR to obtain resolution among nearby resonances with similar shifts and large dipole splittings. Figure 3 contains the two-dimensional separated local field[27] overtone spectrum of *N*-acetylvaline. This spectrum demonstrates resolution of the second-order shifts in one dimension and the corresponding heteronuclear dipole splittings in the second dimension. Figure 4 compares the measurements of the N–H dipole coupling from the fundamental and overtone spectra. The fundamental measurement uses a conventional undecoupled one-dimensional

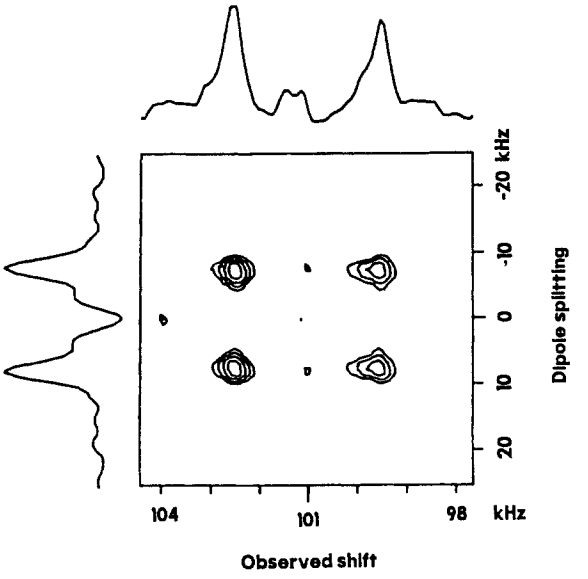

Figure 3. Two-dimensional separated local field overtone spectrum of *N*-acetylvaline. The projection of peaks onto the horizontal axis gives the total observed shift (twice the second-order quadrupole shift plus twice the chemical shift). The projection onto the vertical axis gives a doublet for each nitrogen site, split by the N–H dipole coupling. Observed shifts are thereby correlated with dipole splittings. The spectrum has been symmetrized in the dipolar dimension due to the inherent symmetry of dipolar spectra and in order to generate a pure absorption mode spectrum.

spectrum while the overtone measurement uses a section of the two-dimensional separated local field spectrum. As expected, the two spectra show doublets with splittings differing by a factor of two.[23] This is because the overtone spectra result from $\Delta m \simeq 2$ transitions, whereas the fundamental spectra result from $\Delta m \simeq 1$ transitions. The two measurements yield the same magnitude for the dipole coupling and, in turn, the same angles for the N–H bonds relative to the magnetic field. The values for the quadrupole splittings, observed frequency shifts, and N–H dipole splittings for both inequivalent molecules of *N*-acetylvaline are summarized in Table I.

^{14}N overtone NMR offers an additional orientationally dependent parameter. Since overtone transitions are allowed only because of the quadrupole interaction, the transition probability depends on the orientation of the quadrupole tensor. The transition probability can be measured experimentally as the nutation frequency or the inverse of the 2π pulse length of the overtone transition under rf irradiation. For reasons of sensitivity this is best accomplished by using a variation of the cross-polarization pulse sequence as shown in Figure 5. The measurement is illustrated for the two overtone resonances from the *N*-acetylvaline single crystal. The nutation frequency measurement can be calibrated by measuring the 2π pulse length of a fully allowed transition at a nearby frequency with the same probe and rf power. The nutation frequency values listed in Table I are relative to the

(25) Anderson, A. G.; Hartmann, S. R. *Phys. Rev.* **1960**, *128*, 2023–2041.
(26) Harbison, G. S.; Jelinski, L. W.; Stark, R. E.; Torchia, D. A.; Herzfeld, J.; Griffin, R. G. *J. Magn. Reson.* **1984**, *60*, 79–82.
(27) Hester, R. K.; Ackerman, J. C.; Neff, B. L.; Waugh, J. S. *Phys. Rev. Lett.* **1976**, *36*, 1081–1083.

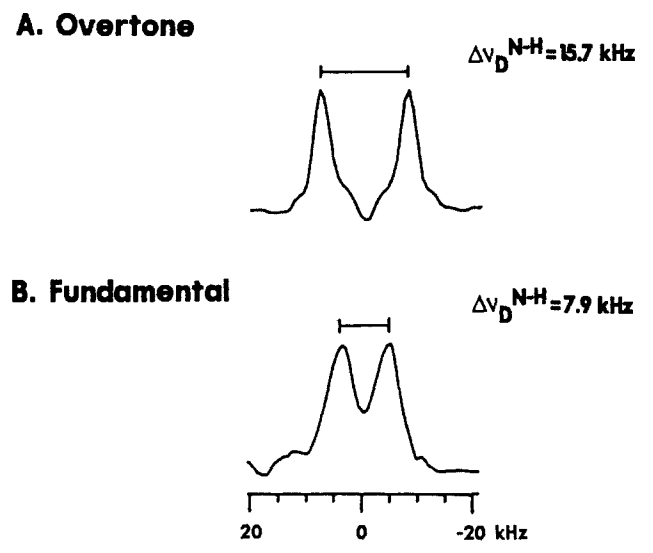

Figure 4. Comparison of the N–H dipole splittings seen in fundamental and overtone spectra. Doublets for molecule M1 are shown, representing dipole splittings in two-dimensional overtone (A) and one-dimensional undecoupled fundamental (B) spectra. The splitting of the overtone resonance is twice as large as the splitting of the fundamental resonances.

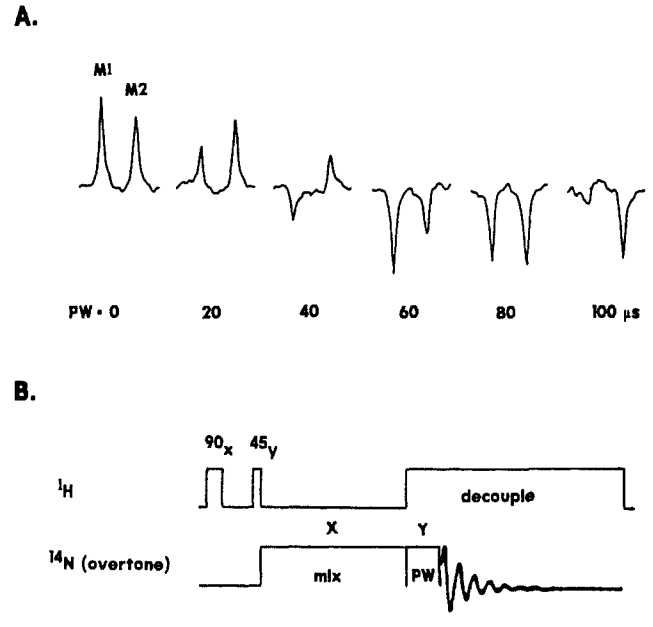

Figure 5. Measurement of overtone nutation frequencies. Overtone spectra in part A are generated with the pulse sequence in part B. Following cross-polarization from proton dipolar order, a phase-shifted overtone rf pulse is applied for a time PW before the overtone signals are acquired. This pulse causes a nutation of the overtone polarization, leading to the oscillatory dependence of the intensities in part A on PW. An overtone peak is nulled whenever PW is an odd multiple of the $\pi/2$ pulse length. The nutation frequency differs between the two peaks because of its dependence on molecular orientation.

nutation frequency of ^{2}H, which had a 2π pulse length of 10.4 μs.

Discussion

Given the established magnitudes of the principal values and the orientation of the principal axes with respect to the molecular frame for the ^{14}N quadrupole tensor[11,18,28] the orientations of the peptide planes can be determined from the data presented in Figures 1–5 and Table I. Figure 6 shows the orientation of the principal axes of the ^{14}N quadrupole interaction tensor in the molecular frame of a peptide plane and defines the polar angles α and β that specify the direction of the static magnetic field. Figure 7 illustrates the orientational dependence of the four spectroscopic parameters: quadrupole splitting $\Delta\nu_Q^{(1)}$, second-order quadrupole shift $\nu_Q^{(2)}$, relative overtone nutation frequency $\nu_{nut}^{(rel)}$, and N–H dipole splitting $\Delta\nu_D^{N-H}$. For clarity, only a single case is shown with the angle $\alpha = 0°$ and the angle β varying between 0 and 90°. The orientational dependences of the four parameters are given explicity by

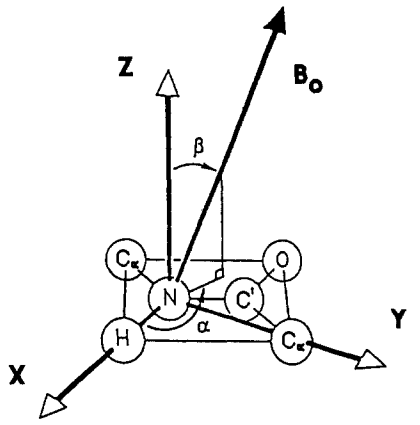

Figure 6. Orientation of the principal axes of the ^{14}N quadrupole interaction tensor with respect to the molecular framework of a peptide plane. The polar angles α and β define the direction of the applied magnetic field B_0. Overtone and fundamental ^{14}N NMR experiments are used to determine α and β for individual peptide planes.

$$\Delta\nu_Q^{(1)} = 3\nu_Q[(3\cos^2\beta - 1) + \eta\cos 2\alpha\sin^2\beta] \quad (1)$$

$$\nu_Q^{(2)} = [\nu_Q^2/(2\nu_0)](|f(\alpha,\beta)|^2 + |g(\alpha,\beta)|^2) \quad (2)$$

$$\nu_{nut}^{(rel)} = (2\gamma_N/\gamma_D)(\nu_Q/\nu_0)|f(\alpha,\beta)| \quad (3)$$

$$\Delta\nu_D^{N-H} = (\gamma_N\gamma_H h/r^3)(3\cos^2\alpha\sin^2\beta - 1) \quad (4)$$

where $\nu_Q = e^2qQ/4h$, ν_0 is the ^{14}N Larmor frequency, γ_N, γ_D, and γ_H are the ^{14}N, ^{2}H, and ^{1}H gyromagnetic ratios, e^2qQ/h and η are the quadrupole coupling constant and asymmetry parameter, r is the N–H bond distance, and $f(\alpha,\beta)$ and $g(\alpha,\beta)$ are given by

$$f(\alpha,\beta) = 3\sin\beta\cos\beta - \eta(\cos 2\alpha\sin\beta\cos\beta + i\sin 2\alpha\sin\beta)$$

$$g(\alpha,\beta) = (3/2)\sin^2\beta + \eta[\cos 2\alpha(1 + \cos^2\beta)/2 + i\sin 2\alpha\cos\beta]$$

Assuming that the chemical shift anisotropy tensor is axially symmetric and that the unique axis is aligned with the N–H bond, the orientational dependence of the chemical shift ν_{cs} is described by

$$\nu_{cs} = \sigma_\parallel\sin^2\beta\cos^2\alpha + \sigma_\perp(1 - \sin^2\beta\cos^2\alpha) \quad (5)$$

where $\sigma_\parallel$ and $\sigma_\perp$ are the principal values of the chemical shift anisotropy tensor.

Through eq 1–5, each experimental measurement places a constraint on the possible orientations of each peptide plane. The constraint for an individual measurement can be conveniently visualized by plotting the combinations of α and β that are consistent with the measurement as a region in the $\alpha\beta$ plane. Plots of this type are shown in Figures 8, 9, and 10. If the experimental measurements are taken to be exact and the coupling constant values are also known exactly, then the corresponding regions consist of lines in the $\alpha\beta$ plane. This is shown in Figure 8A for the case of the measurement of the total frequency shift of molecule M1 in the overtone spectrum. In practice however there are two sources of uncertainty in the analysis of the experimental measurements. One source is uncertainty inherent in the spectra themselves due to such factors as finite line widths, limited resolution, and the presence of noise. The other source is uncertainty in the values of the coupling constant parameters, such as e^2qQ/h,

(28) Sadiq, G. F.; Greenbaum, S. G.; Bray, P. J. *Org. Magn. Reson.* **1981**, *17*, 191–193.

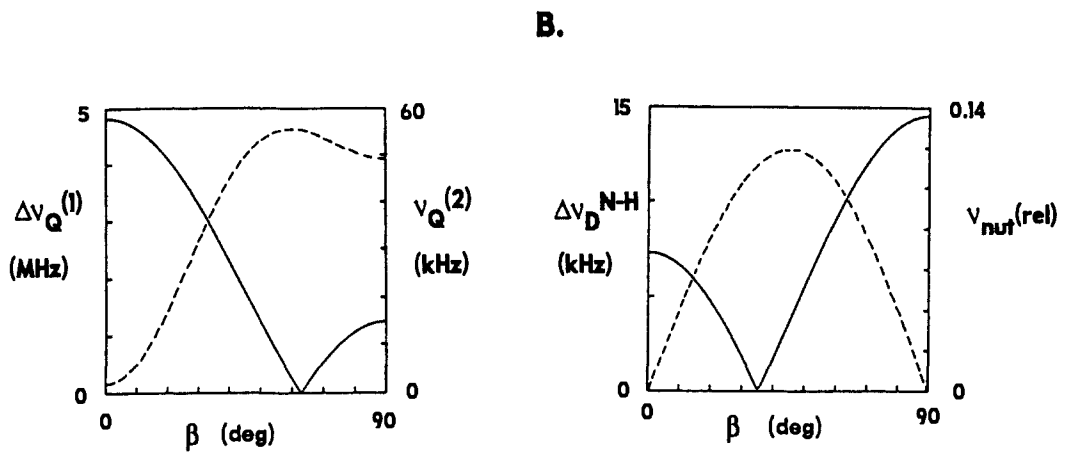

Figure 7. Orientational dependence of the spectroscopic parameters. The dependence on β is shown for the case $\alpha = 0°$. Part A shows the orientational dependence of the quadrupole splitting $\Delta\nu_Q^{(1)}$ (solid line) and the second-order quadrupole shift $\nu_Q^{(2)}$ (dashed line). Part B shows the orientational dependence of the N–H dipole splitting $\Delta\nu_D^{N-H}$ of the fundamental resonances (solid line) and the relative overtone nutation frequency $\nu_{nut}^{(rel)}$ (dashed line).

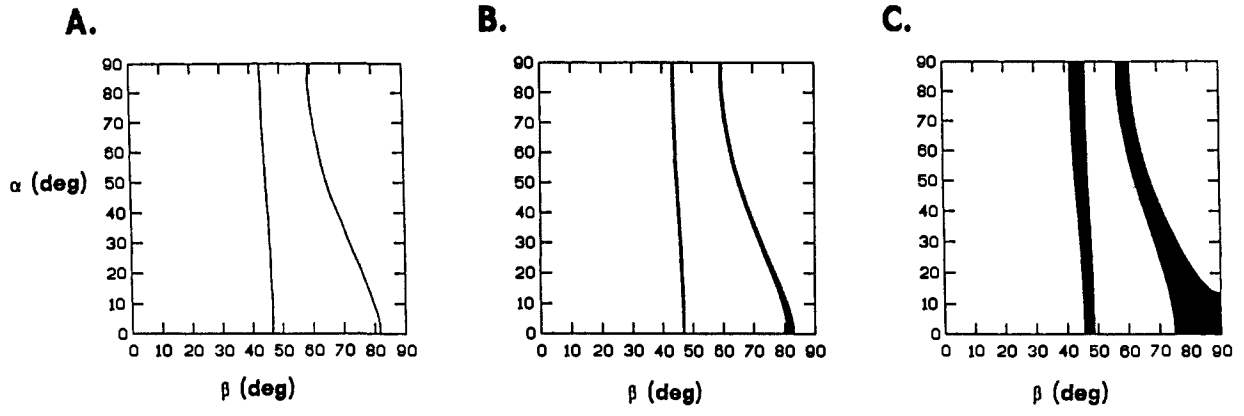

Figure 8. Graphical method for displaying the constraints on a molecular orientation imposed by a spectroscopic measurement. The constraints are seen as regions in the $\alpha\beta$ plane representing the combinations of α and β that are consistent with the measurement. The example shown is for the measurement of the total observed shift of the overtone resonance of molecule M1. (A) The shift is taken to be exactly 103 kHz, and the values e^2qQ/h = 3.21 MHz and η = 0.30 are used. The allowed combinations of α and β appear as lines in the $\alpha\beta$ plane. (B) The shift is allowed to range between 102.5 and 103.5 kHz to account for experimental errors. (C) e^2qQ/h is allowed to range between 3.18 and 3.24 MHz and η is allowed to range between 0.27 and 0.32 to account for uncertainties in the coupling constants. In A, B, and C, the values $\sigma_\parallel$ = 114 ppm and $\sigma_\perp$ = −57 ppm are used for the chemical shift principal elements.

η, and r, and in the orientation of the interaction tensors with respect to the molecular frame. The coupling constants and tensor orientations are typically measured on model compounds, but they are expected to vary somewhat in going from a model compound to the molecule of interest as a result of slight differences in the chemical and crystal environments and, possibly, differences in the influence of molecular motion. Either source of uncertainty in the analysis can be taken into account by establishing upper and lower limits both on the coupling constants and on the experimental measurements and by plotting the combinations of α and β that are consistent with those limits. Figure 8B shows the regions of α and β combinations that are consistent with the frequency shift measurement allowing for experimental uncertainty due to the overtone line widths and due to uncertainty in the $2\nu_0$ reference. Figure 8C shows the regions of α and β combinations that are consistent with the total observed shift measurement allowing for uncertainty in e^2qQ/h and η. The limits on the values of the quadrupole coupling parameters are chosen to reflect the variation of reported values for *N*-acetylvaline determined by NQR,[28] single crystal rotation studies,[11] and the analysis of overtone powder patterns.[18] It is apparent in Figure 8 that the uncertainty in the analysis of the total observed shifts is dominated by uncertainty in the coupling constants that characterize the quadrupole interaction. For other fundamental and overtone spectroscopic measurements, uncertainty in the analysis may be primarily a result of experimental imprecision or may have substantial contributions both from experimental imprecision and from uncertainty in the coupling constants and tensor orientations.

Figure 9 contains plots that display the constraints on α and β imposed by each individual experimental measurement on molecule M1. For each measurement, variation around the values given in Table I and variation in the coupling constants that enter into eq 1–4 is allowed as discussed above. The fact that the allowed combinations of α and β are different for each experimental measurement indicates that each measurement provides an independent constraint on the peptide plane orientation. The similarity of the allowed regions for the quadrupole splitting and for the total observed shift measurements is a consequence of the relation

$$(\Delta\nu_Q^{(1)})^2 = -24\nu_0\nu_Q^{(2)} + 36\nu_Q^2 + 12\nu_Q^2\eta^2 \qquad (6)$$

The actual orientation of a peptide plane must satisfy all of the independent constraints. Therefore, that orientation must correspond to a point in the $\alpha\beta$ plane that lies within the intersection of the allowed regions determined by the individual measurements. Figure 10A shows the intersection of the allowed regions determined by the ^{14}N overtone NMR measurements. Figure 10B shows the interaction of the allowed regions determined by the fundamental measurements. Finally, Figure 10C shows the intersection of the allowed regions determined by all measurements, i.e., the combinations of α and β that are consistent with all of the experiments. A single allowed region is seen in Figure 10C, corresponding to $\alpha = 88 \pm 2°$ and $\beta = 42.5 \pm 0.5°$. Thus, by combining a series of independent orientational mea-

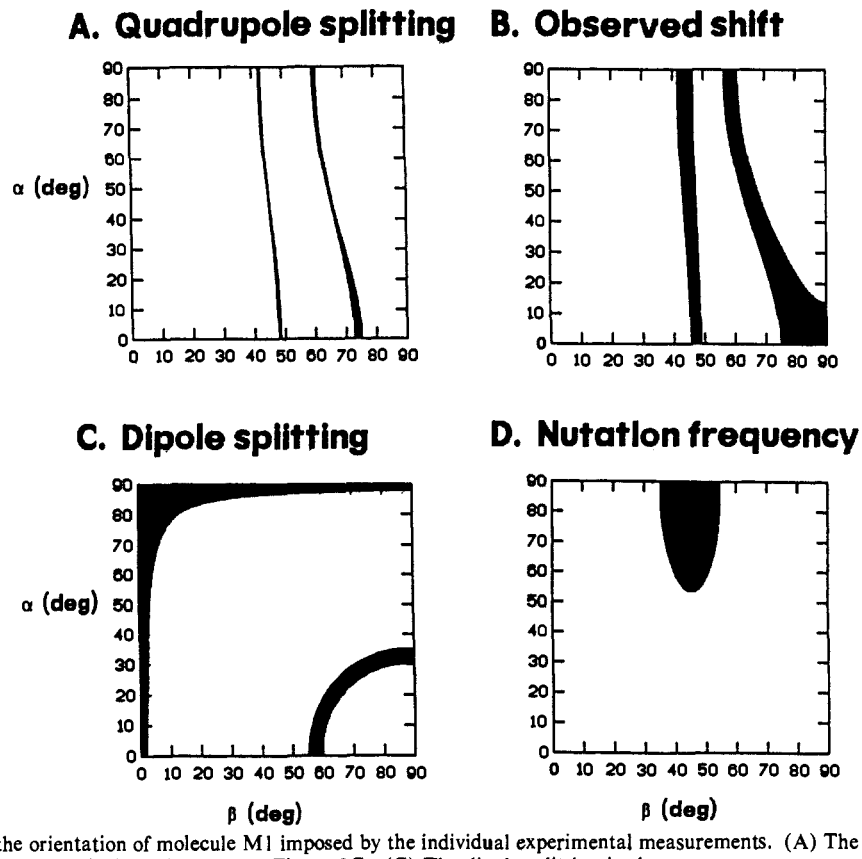

Figure 9. Constraints on the orientation of molecule M1 imposed by the individual experimental measurements. (A) The quadrupole splitting ranges between 1.181 and 1.201 MHz, and (B) is the same as Figure 8C. (C) The dipole splitting in the overtone spectrum ranges between 14.9 and 16.5 kHz. (D) The relative nutation frequency varies between 0.070 and 0.073. In A, B, C, and D, e^2qQ/h ranges between 3.18 and 3.24 MHz, η ranges between 0.27 and 0.32, and r ranges between 1.05 and 1.09 Å.

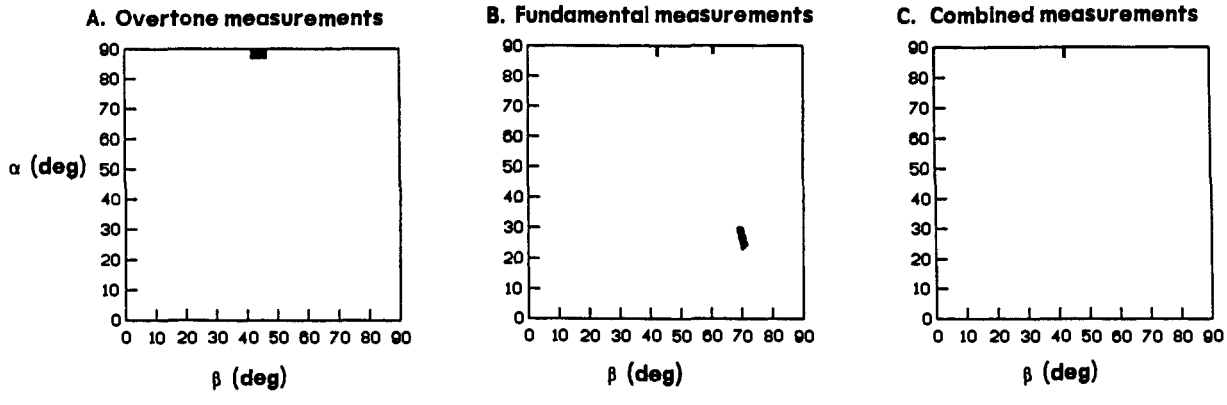

Figure 10. Combinations of α and β for molecule M1 that are consistent with the overtone dipole splitting, observed shift, and nutation frequency measurements (A), the fundamental dipole splitting, observed shift, and quadrupole splitting measurements (B), and the combination of all overtone and fundamental ^{14}N NMR measurements (C). The measurement of multiple orientationally dependent parameters leads to a small final region in the $\alpha\beta$ plane that represents the orientation of the peptide plane.

surements, a final orientation is determined precisely. The same procedure applied to molecule M2 yields $\alpha = 89 \pm 1°$ and $\beta = 62.5 \pm 0.5°$. The orientations determined for both molecules are depicted in Figure 11.

The peptide plane orientations are determined uniquely for $0 < \alpha < 90°$ and $0 < \beta < 90°$, the portion of the $\alpha\beta$ plane shown in Figures 8, 9, and 10. However, to absolutely define the orientation of a peptide plane with respect to the magnetic field vector requires α between 0 and 360° and β between 0 and 180°. It is apparent in eq 1–5 that if α were replaced by $180° - \alpha$, $180° + \alpha$, or $360° - \alpha$ or if β were replaced by $180° - \beta$, the same experimental measurements would result. Therefore, the NMR measurements give eight symmetry related orientations for each peptide plane. The ambiguities arise because the N–H bond direction coincides with the x axis of the quadrupole tensor. Additional measurements can reduce the number of possible orientations. For example, a measurement of either the C_α–N

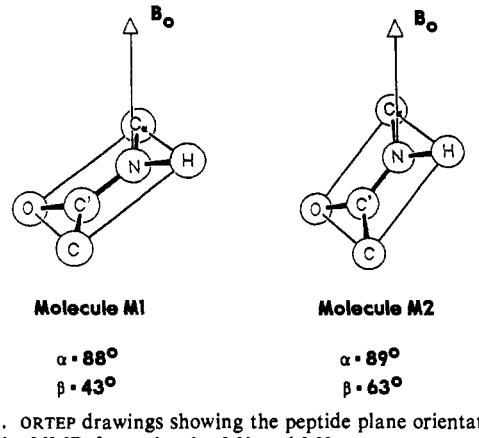

Figure 11. ORTEP drawings showing the peptide plane orientations determined by NMR for molecules M1 and M2.

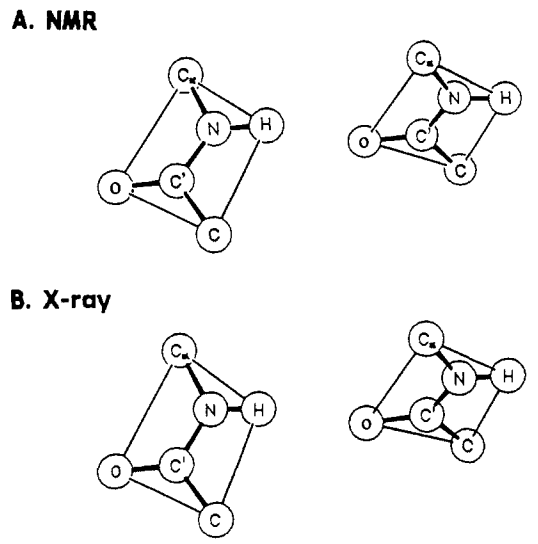

Figure 12. A comparison of the NMR plane orientations and the X-ray diffraction structure. (A) The NMR plane orientations are rotated around the magnetic field vector and translated to give maximum overlap with the X-ray diffraction orientations. (B) Two magnetically inequivalent peptide planes in the unit cell are shown.

or the C′–N dipole couplings, with a ^{13}C labeled C_α or C′ nucleus, would reduce the number of possible plane orientations to four.

The crystal structure of *N*-acetylvaline has four molecules in the unit cell with two pairs of molecules related by a center of inversion.[29] NMR parameters are invariant to inversion, and thus only two different molecular orientations are observed. One of the inversion pairs corresponds to molecule M1 and the other to M2. The peptide plane orientations determined by NMR can be compared to the X-ray crystal structure in the following manner. For each of the eight possible α, β combinations of molecule M1, the α and β angles can be calculated for molecule M2 by using the crystal coordinates. For the $360° - \alpha$, β combination of M1 the agreement between the calculated and experimental NMR angles is excellent. The angles $\alpha = 89°$ and $\beta = 117.1°$ are calculated and after taking the supplement of β, 62.9°, they fall within the NMR experimental ranges for M2.

The NMR and X-ray diffraction results are compared in Figure 12. The NMR plane orientations which agree with the crystal structure are shown in Figure 12A. The orientations of two magnetically inequivalent planes in the unit cell as determined by X-ray diffraction are shown in Figure 12B. The two NMR planes were rotated around the magnetic field vector and translated with respect to each other to give the maximum overlap with the X-ray structure. The two planes from the crystal structure are shown with the calculated magnetic field vector aligned along the magnetic field vector of the NMR planes.

We have shown how fundamental and overtone ^{14}N NMR measurements of the quadrupole splitting, second order quadrupole shift and chemical shift, N–H heteronuclear dipole splitting, and overtone nutation frequency can be combined to determine the orientations of the two magnetically inequivalent molecules in a *N*-acetylvaline single crystal. All the measurements were carried out for a single arbitrary crystal orientation. The results on the model peptide crystal indicate the potential of ^{14}N NMR for structural studies of polypeptides and proteins.

These methods can be applied to determining the orientations of other chemical groups that contain nitrogen. Since all NMR measurements are unaffected by reversing the direction of the applied static magnetic field, there will always be at least two orientations that are consistent with the measurements, related by replacing α with $180° + \alpha$ and β with $180° - \beta$. For a chemical group in which the N–H bond direction does not coincide with one of the principal axes of the quadrupole tensor or lie in a plane determined by two of the principal axes, then the orientation of that group can be determined uniquely up to a reversal of the field direction. In certain cases, the ambiguity in orientation can be eliminated by additional knowledge about the molecule of interest. For example, ^{14}N NMR measurements may be useful for determining the precise orientations of purine and pyrimidine base pairs in nucleic acid fibers, where the approximate orientations are known from diffraction studies. In the case of a polypeptide, adjacent peptide planes are joined at C_α atoms, and orientations that are not compatible with tetrahedral coordination at the shared C_α can be ruled out. Steric interference involving amino acid side chains and secondary and tertiary backbone structures can further reduce the number of possible orientations.

A simple method for analyzing the experimental data and for including effects of uncertainties in the measurements and in the nuclear spin couplings has been presented. This method of analysis is applicable to any solid state NMR study of molecular orientation. The experimental techniques and data analysis are not restricted to single crystal samples but may be applied to any system in which there is at least one direction of orientation. Such systems include oriented membranes, liquid crystals, fibers, and magnetically oriented particles.

Acknowledgment. We thank P. Carroll for determining the crystal structure of *N*-acetyl-D,L-valine by X-ray diffraction. This research is being supported by Grants (GM-24266 and GM-29754) from the N.I.H. R.T. acknowledges support from Damon Runyon-Walter Winchell Cancer Fund Fellowship DRG-891. P.L.S. is supported by a National Science Foundation Graduate Fellowship.

Registry No. *N*-Acetyl-DL-valine, 3067-19-4.

(29) Carroll, P., private communication.